

STATUS OF CHIRPED PULSE LASER SHAPING FOR THE PITZ PHOTOINJECTOR

C. Koschitzki*, J. Good, M. Gross, Y. Chen, G. Loisch,
M. Krasilnikov, R. Niemczyk, F. Stephan, DESY Zeuthen, Germany
L. Winkelmann, T. Lang, DESY Hamburg, Germany
S. Mironov, E. Khazanov, IAP RAS Nischni Nowgorod, Russia

Abstract

In this publication we show the current status on spectral-spatial shaping of laser pulses at the Photo Injector Test facility at DESY-Zeuthen (PITZ) for providing temporally and spatially variable laser pulse intensities at a photo injector cathode. The temporal and spatial distribution of these laser pulses will determine the properties of the emitted electron bunch, which will influence the properties of Free-Electron Laser (FEL) radiation, after these electron bunches are further accelerated in the linac. The presented pulse shaper modulates the spectral amplitude of a chirped pulse with the additional capability to transversely vary the pulse shape, thus allowing a three dimensional pulse shaping. However, these pulses are particularly difficult to convert to shorter wavelength in nonlinear crystals preserving their shape. Shaping components like the spatial light modulator are not available for the required UV radiation and thus a specialized conversion setup had to be built, utilizing angular chirp matching and imaging to achieve shape preservation. In this work we present preliminary results of laser pulses shaped in the infrared and the similarity to their converted ultraviolet counterparts.

INTRODUCTION

Free-Electron Lasers (FEL) are currently the most powerful source for coherent x-rays. They are typically driven by a linear electron accelerator, which as opposed to ring type accelerators, preserves electron bunch properties from its injector source. Thus the performance of photo injectors is studied at PITZ. The initial temporal and spatial distribution of the electron bunch is determined by the shape of the laser pulse used to emit electrons from the photo cathode via the photo electric effect. As laser amplifiers for short-pulse amplification with high average power output are only available for infrared (IR) wavelength, it is necessary to use harmonic generation processes in nonlinear crystals to convert the laser pulses to the ultraviolet (UV) in order to overcome the work function of the photo cathode material. In this case this is a dicaesium telluride (Cs_2Te) with a vacuum threshold energy of 3.5 eV or 354 nm. Two consecutive second harmonic generation (SHG) processes are applied to get to the fourth harmonic of a 1030 nm IR laser and thus 257 nm or 4.8 eV. UV optical components needed for the shaper are either not available, very expensive or inefficient at these wavelength ranges. Thus laser pulse shaping is done in IR

and special care has to be taken to preserve pulse shapes through the conversion process. In particular the conversion from visible (VIS) to UV light is challenging. A laser pulse shaper capable of shaping in three dimensions, i.e. spatially and temporarily, has been developed at PITZ, based on a prior system by Mironov et al. [1]. Preserving such pulses in all three dimensions through the conversion process is a key challenge in order to use the pulse shaper system for the photo injector application. Mironov et al. have proposed and simulated a method for shape preserving conversion [2], using an angular chirp matching with type I phase matching. In this work preliminary experimental results will be shown.

SLM PULSE SHAPER

The most prominent scheme to alter the laser pulses temporal distribution from its typical Gaussian shape is the coherent pulse stacking technique, in which copies of short laser pulses are delayed, attenuated and recombined. The precision depends on the amount of copies produced. Such a system is also operated at PITZ [3]. Spatial shaping is added by masking the transverse distribution typically by a round aperture after the laser pulses have longitudinally been shaped in IR and converted to UV. The dispersive pulse shaper, as proposed and demonstrated by Mironov et al. [1], uses a principle very similar to a spectrograph. The beam is focused into a line onto a spatial light modulator (SLM) by a cylindrical lens, where the spread out spatial dimension can be modulated. Perpendicular to the line focus the beam is dispersed by an optical grating, allowing for a simultaneous modulation of one spatial dimension and the spectrum. The beam path is then reversed to undo the cylindrical focusing and the dispersion (see Figure 1). SLMs can shift the laser phase on each of its pixels between 0 and 2π . The phase shifting of the SLM is polarization dependent, so one can apply quarter $\frac{1}{4}\lambda$ plates and a polarizer in order to turn the phase shift into a spatial-spectral attenuation. Without the $\frac{1}{4}\lambda$ plates the shaper can be operated as variable prism as shown in section . As a single shaper allows only access to one spatial dimension, the beam is rotated by 90 degrees and the shaping process is repeated. Thus the 3D spectral-spatial attenuation function $f_a(x, y, \lambda)$ is not fully arbitrary, but must fulfill the condition

$$f_a(x, y, \lambda) = f_1(x, \lambda) * f_2(y, \lambda). \quad (1)$$

This condition results in 3D shaped pulses consisting of rectangular spatial profiles along the wavelength axis. In order to achieve a targeted attenuation of the laser pulse

* christian.koschitzki@desy.de

Content from this work may be used under the terms of the CC BY 3.0 licence (© 2019). Any distribution of this work must maintain attribution to the author(s), title of the work, publisher, and DOI

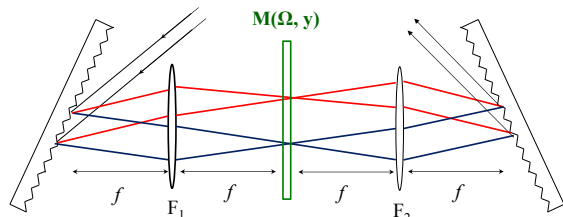


Figure 1: Schematic of an SLM based shaper.

we diagnose the beam using a slit spectrograph. With correct imaging from the SLM to the spectrograph plane we can detect the laser distribution as on the SLM plane and apply a targeted attenuation. Thus we obtained an evenly filled rectangle on the spectrograph as shown in Figure 2 b). This beam moved within 12 hours by less than one pixel on the spectrograph, i.e. shows excellent position stability. Simultaneous shaping by both SLMs can be recovered by scanning the position of the entrance slit of the spectrograph (2 d). The spatial-temporal distribution can be obtained from the spatial-spectral distribution by Fourier transformation along the spectral axis considering the chirp or group delay dispersion (GDD).

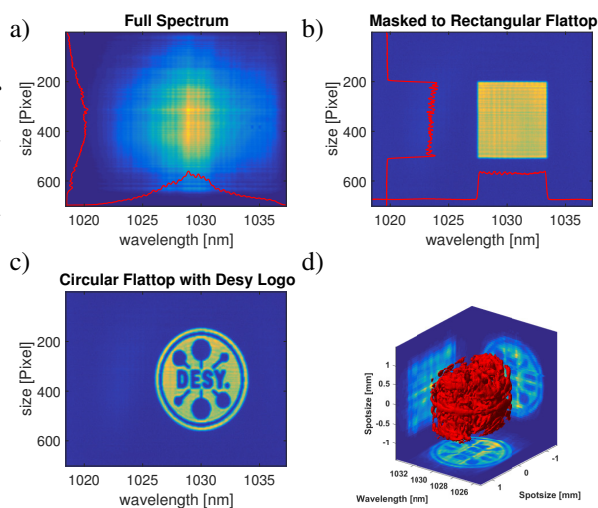


Figure 2: Spectrograph images of the shaped laser pulse. a) unshaped pulse b) Rectangular flattop c) Circular flattop with Desy logo d) Desy logo on both SLMs retrieved by spectrograph slit scan (vertical resolution).

CONVERSION

Second harmonic conversion output of nonlinear crystals depends on the square of the laser pulse intensity. When working with low laser intensities, focusing the laser pulse on the conversion crystal is the typical approach. The focal distribution of a laser pulse corresponds to the Fourier transform of its collimated spatial distribution. High spatial

frequency features, i.e. sharp edges, become low intensity features around the focal spot and will be strongly suppressed due to the non-linearity of the conversion. Thus the conversion acts like a spatial filter. It can be seen that this is also the case for temporal transform limited pulses. Thus the spatially modified laser pulses have to be imaged into the conversion crystal uncompressed. As the intensity is lower than in the focused case, the efficiency will be reduced. Another problem is the phase matching, as for a type I critical phase matching setup only a limited bandwidth is supported in the conversion process. J.P. Torres et al. [4] have proposed a method for broadband phase matching, where an angular chirp (AC) is introduced to match the wavelength dependent phase matching angle. Mironov et al. [2] have shown a numerical method to simulate the nonlinear SHG processes with chirp matching for picosecond laser pulses with high numeric efficiency. The simulation results match those obtained by a more general applicable, but slower tool developed by Lang et. al [5].

The current setup operates with a 4 mm LBO crystal at beam intensities of approximately 2.5 GW cm^{-2} and a 0.5 mm thick BBO crystal at 1.5 GW cm^{-2} . The required AC for broadband matching in the LBO is generated by 2 SF11 prisms with an AC of 0.065 mrad/nm each and magnified by a transport telescope with $M=8.9$ to the required AC of 1.15 mrad/nm for the LBO. The combined origin of dispersion must be aligned to coincide with the image plane of the spatial modulation in order to avoid spatial dispersion in the image plane inside the conversion crystal. To achieve AC matching inside the BBO crystal the existing dispersion from the LBO can be magnified using an intermediate transport telescope between LBO and BBO crystal. Finally, the setup contains a variable three-lens telescope imaging the shaper output to the SF11 prisms in order to vary the beam size on the crystal. Figure 3 shows how a spatial attenuation from the shaper can be retrieved in the UV. In one dimension sharp profiles can be maintained, while in the other direction features are smeared out, owing to the spatial walk-off between fundamental and harmonic beam inside the conversion crystal. This effect is proportional to the crystal thickness. The nonlinear conversion is expected to reduce the width of a gaussian beam by approximately a factor 4, due to nonlinear correlation between input and output profile.

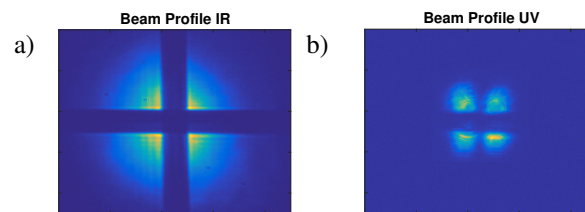


Figure 3: Beam Images in IR. a) and UV b) with spatial line masks from both SLMs. Horizontal smearing is due to spatial walkoff from the BBO crystal.

ANGULAR CHIRP DEPENDENCE

The aforementioned simulation tools ([2], [5]) allows us to simulate the effects of mismatched AC on the conversion efficiency. At the same time the shaper setup can be used to scan this dependence experimentally. For this we have to use the SLM in phase shifting mode without the $\frac{1}{4}\lambda$ plates. By varying the phase shift θ linearly along a spatial dimension x for a given wavelength λ , one applies a deflection angle ϕ to that part of the spectrum

$$\phi = \lambda \frac{\delta\theta}{\delta x}. \quad (2)$$

By also varying this angle along the wavelength axis of the SLM an AC $\delta\phi/\delta\lambda$ is generated. The additional benefit is that the origin of dispersion is at the SLM, which by image transport is moved to the crystal plane, as detailed above. Thus spatial dispersion is minimized and only angular dispersion is generated at the plane of the crystal. The total magnification of the image system from the SLM to the crystal plane has to be considered in order to obtain the AC at the crystal plane from the AC generated at the SLM. In Figure 4 the relative beam energy normalized to the maximum energy and the spectral width are shown as a function of applied angular chirp. The beam energy has been measured using the camera integral of the UV profile camera as in Figure 3. Simulation predicts a conversion efficiency of 0.4 % for this Gaussian beam with 10 ps FWHM pulse duration and 10 μJ pulse Energy, corresponding to a peak intensity of 3.75 GW/cm^2 . In Figure 5 the simulated conversion efficiency is plotted as function of AC for different energies. Absolute pulse energy measurement for the output UV pulses was not available at the time. Spectral width of the output beam has been measured with a UV spectrograph. This experiment demonstrates the importance of the achieved broadband phase matching. As only a fraction of the spectrum, that the shaper is supposed to modulate, would be converted in an unmatched scenario, the temporal structure could not be maintained if no angular chirp is applied to the nonlinear conversion.

CONCLUSION

This paper shows that the SLM shaping approach will provide a stable, versatile and precise method for pulse shaping of infrared laser pulses. The matched angular chirp conversion shows promising results to maintain the pulse shape through the conversion process while reaching satisfying conversion efficiency. In the next step more complex shaping needs to be applied to the infrared pulses, to study the shape preservation and its limitations in detail. In order to get more direct access to the temporal structure, a cross correlator for the IR and a difference frequency cross correlator for the UV pulses are planned. The final goal is to reach homogeneous UV laser intensity distributions of different 3D shapes with as sharp as possible boundaries in all three dimensions.

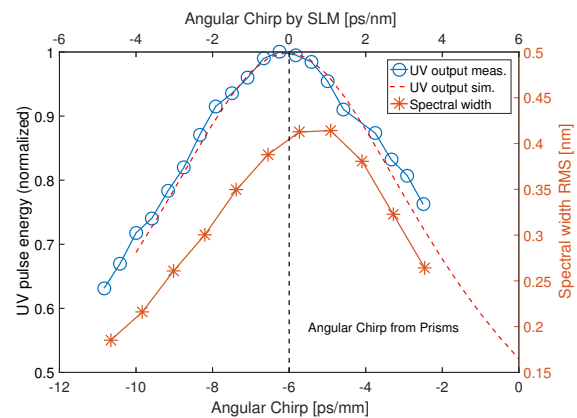


Figure 4: Normalized UV output of conversion section (blue) and spectral width of the UV pulses (orange) as function of applied angular chirp.

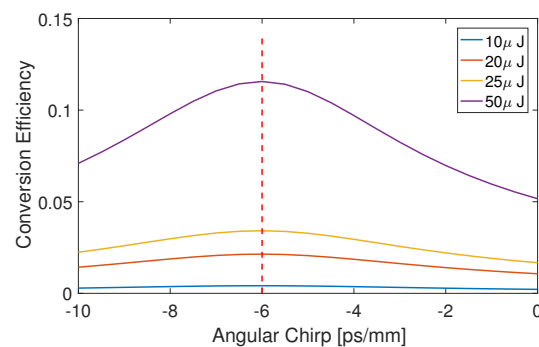


Figure 5: Simulated conversion efficiency for Gaussian beam as function of angular chirp.

REFERENCES

- [1] S. Mironov *et al.*, “Shaping of cylindrical and 3D ellipsoidal beams for electron photoinjector laser drivers”, *Applied Optics*, vol. 55, no. 7, p. 1630-1635, Feb. 2016, doi: 10.1364/AO.55.001630
- [2] S. Mironov *et al.*, “Generation of the second and fourth harmonics with retaining the three-dimensional quasi-ellipsoidal distribution of the laser pulse intensity for a photoinjector”, *Radiophysics and Quantum Electronics*, vol. 61, no. 6, p. 456, Nov. 2018, doi: 10.1007/s11141-018-9907-2
- [3] I. Will *et al.*, “Generation of flat-top picosecond pulses by coherent pulse stacking in a multicrystal birefringent filter”, *OPTICS EXPRESS*, vol. 16, no. 19, p. 14922-14937, Sep. 2008, doi: 10.1364/OE.16.014922
- [4] J. P. Torres *et al.*, “Angular dispersion: an enabling tool in nonlinear and quantum optics”, *Advances in Optics and Photonics*, vol. 2, p. 319-369, May. 2010, doi: 10.1364/AOP.2.000319
- [5] T. Lang *et al.*, “Impact of temporal, spatial and cascaded effects on the pulse formation in ultra-broadband parametric amplifiers”, *OPTICS EXPRESS*, vol. 21, no. 1, p. 949-959, Jan. 2013, doi: 10.1364/OE.21.000949